CHAPTER 3

Synthesis and Characterisation of a Low Band-gap Copolymer Based on DPP and Fused Thieno-TTF Units for Organic Photovoltaics and Organic Field-Effect Transistors

3.1. ABSTRACT

Following an approach developed in this group to incorporate of TTF units in conjugated polymeric systems, a new low band gap polymer **p(DPP-TTF)** has been synthesised *via* Suzuki cross-coupling polymerisation. This polymer is based on a fused thieno-TTF unit which enables the direct annexation of the TTF unit into the polymer and a second co-monomer is based on DPP core. This unit is well-known for showing high absorptions in the UV-visible region of the spectrum. **p(DPP-TTF)** has been fully characterised and its performance in organic filed-effect transistors and organic photovoltaics has been studied.

3.2. SYNTHESIS OF p(DPP-TTF)

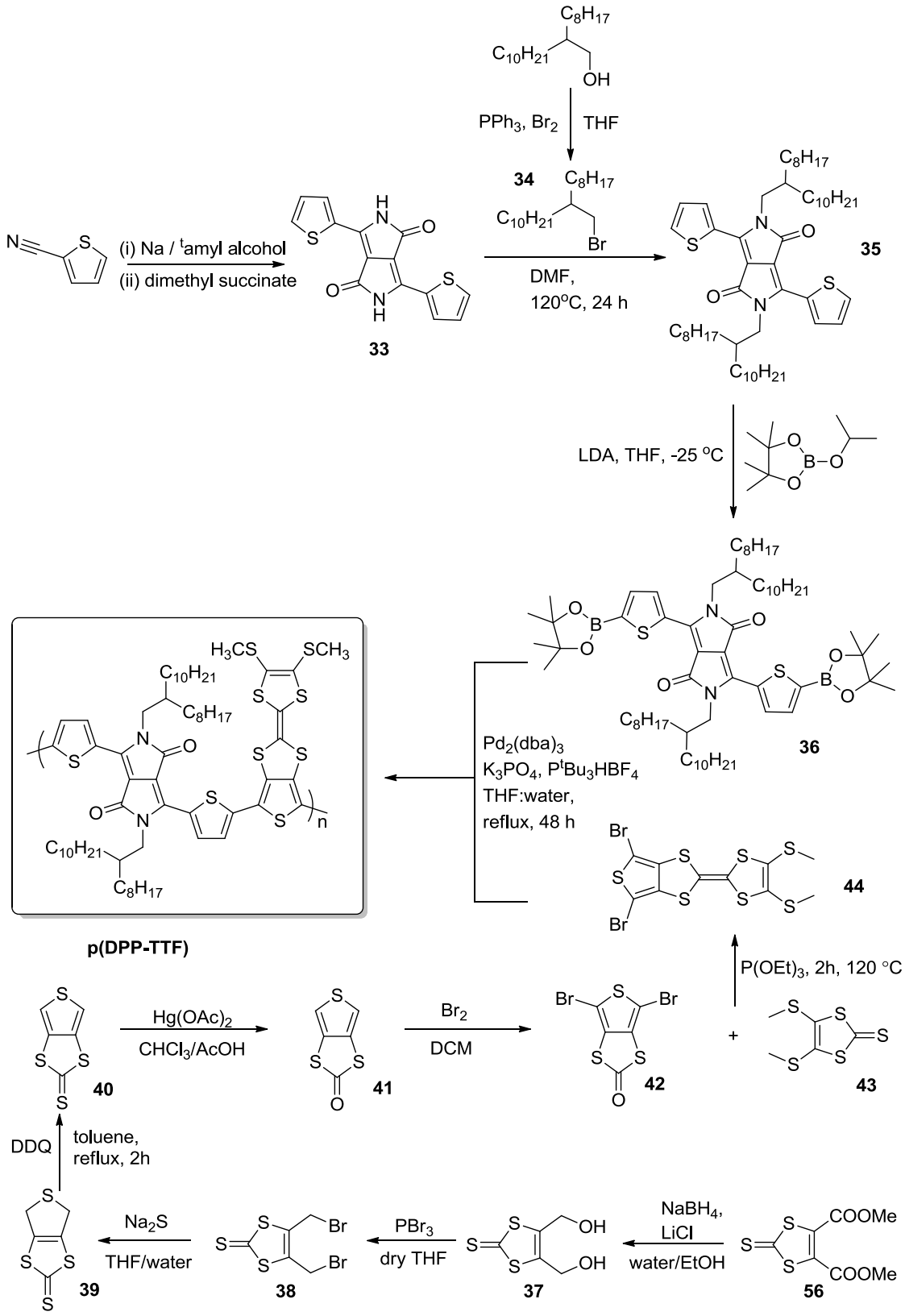

3.3 INTRODUCTION

The work carried out by Wudl *et al.*[1,2] in the early 1970s, based on the synthesis and study of the interesting properties of tetrathiafulvalene (TTF, **45**, Figure 3.1.) and its derivatives, led to the development of a new family of electroactive compounds. The high interest in these materials is due to their capability to act as strong electron-donor compounds.[3,4,5,6] TTF is a pseudo-aromatic, 14 π-electron system in which oxidation to the stable radical cation and dication occurs reversibly at relatively low potentials (E^{o}_{1ox} = +0.34 V; E^{o}_{2ox} = 0.78 V versus Ag/AgCl in acetonitrile).[5] The radical cation and the dication gain aromaticity according to Hückel's rule (4n + 2 π-electrons). Therefore, the aromatisation energy gain, obtained when the neutral molecule is oxidised firstly to the radical cation and secondly to the radical dication, is the primary reason that these compounds are electron-donors. Furthermore, whereas the neutral core in TTF derivatives is often puckered, the oxidised species adopt a planar conformation, which can be interesting when intermolecular stacking is desired.[7] In combination with tetracyano-*p*-quinodimethane (TCNQ, **46**), TTF **45** forms a stable charge transfer salt that was the first organic conductor and shows large conductivity down to 59 K (metallic conductivity).[8]

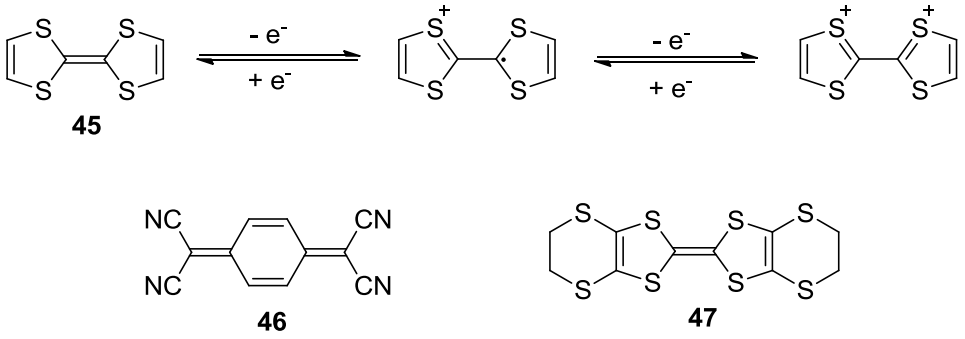

Figure 3.1. TTF (**45**, oxidation-reduction system: neutral molecule, radical cation and dication), TCNQ (**46**) and BEDT-TTF (**47**).

The electron-donating properties of TTF derivatives can be finely tuned by incorporating substituents to the core. Thus, by attaching electron-donating or electron-withdrawing groups to the TTF core, the oxidation potentials can be increased or decreased in comparison to **45** (unsubstituted TTF). Moreover, additional sulfur atoms attached to the TTF unit can enhance higher crystal order. Doubtless, the best example is BEDT-TTF (**47**),[9] which has four additional sulfur atoms, and its salts have shown superconductivity. The extra sulfurs increase the number of interactions between molecules leading to non-covalently connected molecules in the solid state. Additionally, CH···S contacts are very useful to generate secondary interactions.[4] The replacement of the sulfur atoms in TTF and its derivatives by higher chalcogen (*chalkos* (ore) + *gen* (formation), *Greek)* atoms (selenium and tellurium) has been thoroughly studied and superconducting salts have been prepared.[10]

The aforementioned properties and the great versatility for derivitisation make these compounds an interesting building block to be used in materials chemistry. Therefore, many materials with interesting electrochemical properties incorporate a tetrachalcogenafulvalene moiety or an analogue. Their unique electrochemical and structural properties find relevance in areas such as field-effect transistors (FETs),[11,12,13] molecular memory,[14] proton conduction for fuel cell components,[15] new charge storage devices,[16] mechanical molecular switches,[17] electrochromism,[18] sensitized-solar cells,[19] non-linear optics[20] and multi-stimuli-reponsive gels and micelles.[21,22]

3.3.1 Synthesis of TTF and its Derivatives

Although strong acidic conditions and strong oxidising agents can destroy the core, TTFs are generally stable to many synthetic transformations. Since the first synthesis of **45**,[1,23] several synthetic routes have been used to prepare this molecule (see below). On the other hand, the synthetic route to prepare substituted TTF derivatives depends highly on the substituents of the final molecules.[5,6,24,25,26] Some TTF derivatives have been synthesised by double condensation of 1,2-dichalcogenolates

with tetrachloroethylene in the presence of triethylamine,[27] but the method is not robust and low yields are generally obtained.

The most popular synthetic routes to prepare substituted TTFs have 1,3-dichalcogenole rings as key intermediates , which are usually easily prepared.[28,29] These methods can be classified as *selective* or *non-selective* depending on the capacity to produce unsymmetrical TTF derivatives.

The cross-coupling of 1,3-dithiolium salts has been used to prepare TTF derivatives (Scheme 3.1.).[30] The coupling is carried out in the presence of a basic medium *e.g.* tertiary amine which deprotonates the 1,3-dithiolium salts forming a dithiolium carbene. This carbene can either dimerise with another dithiolium carbene or react with the remaining dithiolium salt, followed by deprotonation of the intermediate adduct, to give the unsymmetrical TTF (**48**). Since the carbene can undergo self-coupling, two symmetrical TTFs are usually obtained.

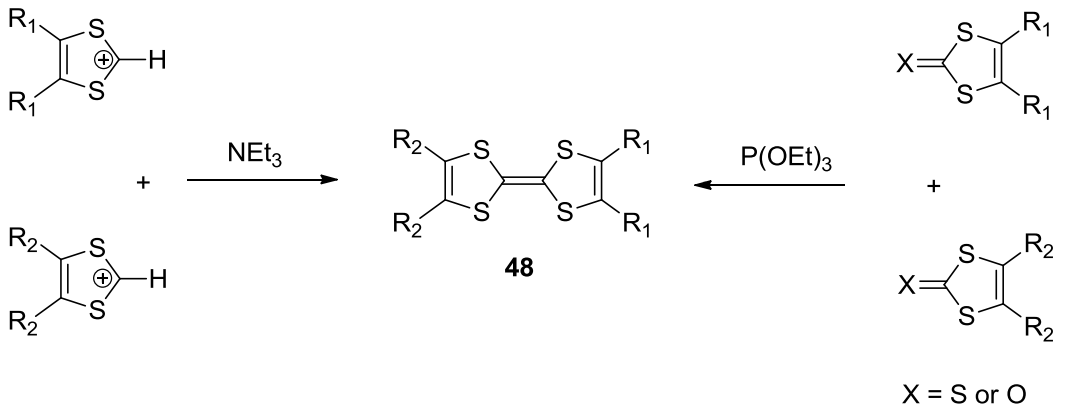

Scheme 3.1. Cross-coupling reaction of 1,3-dithiolium salts and Cross-coupling reaction of 1,3-dichalcogenole-2-chalcogenone.

The most widely used method to synthesise unsymmetrical TTFs is carried out by coupling of 1,3-dichalcogenole-2-chalcogenone (thiones, ones or selenones) mediated by phosphorous reagents (such as phosphines or phosphites) (Scheme 3.1.).[31,24] The nature of the chalcogenone to be coupled, the temperature, the

concentration and the nature of the phosphorous reagent plays a crucial role in the achievement of the reaction.[32] It has been demonstrated that the reaction can be improved when a derivative of oxone is coupled with a different derivative of thione rather than the corresponding oxone.[33] This method is not selective and symmetrical TTFs diminish the yield of the reaction. Additionally, the purification usually requires chromatographic column and the similar R_f of the three main products make it difficult to isolate the desired compound.

Wittig-type condensation to obtain unsymmetrical TTFs was first described by Cava *et al* (Scheme 3.2.).[34] The unsymmetrical TTF is obtained after a condensation between a 1,3-dichalcogenol-2-ylide and a 1,3-dichalcogenol-2-ylium. In this reaction *n*-butyl lithium deprotonates the phosphonium ylide, which reacts with the dithiolium salt. Subsequent deprotonation by a tertiary amine gives the unsymmetrical TTF. However, this reaction is not totally selective and the formation of symmetrical TTFs has been observed.[35,36]

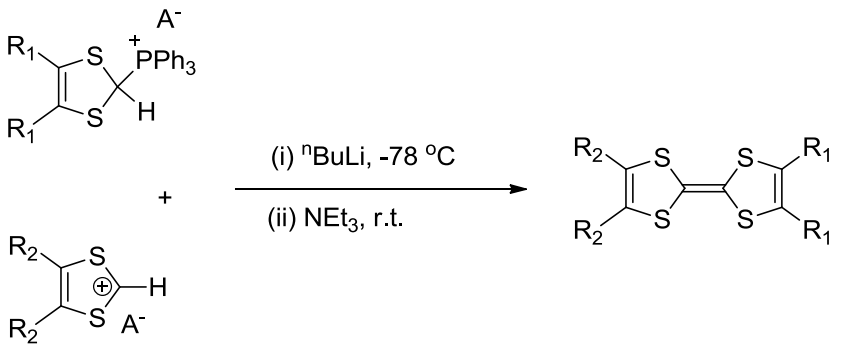

Scheme 3.2. Wittig-type condensation

Lerstrup *et al.*[37] used Horner-Wadsworth-Emmons type condensation methodology to prepare unsymmetrical TTFs selectively with 1,3-dichalcogenole-2-phosphonates (Scheme 3.3.). The phosphonate carbanion generated after deprotonation of 1,3-dichalcogenole-2-phosphonate is thought to react with the piperidyum salt to form an adduct which, after several rearrangements, leads to the unsymmetrical TTF.

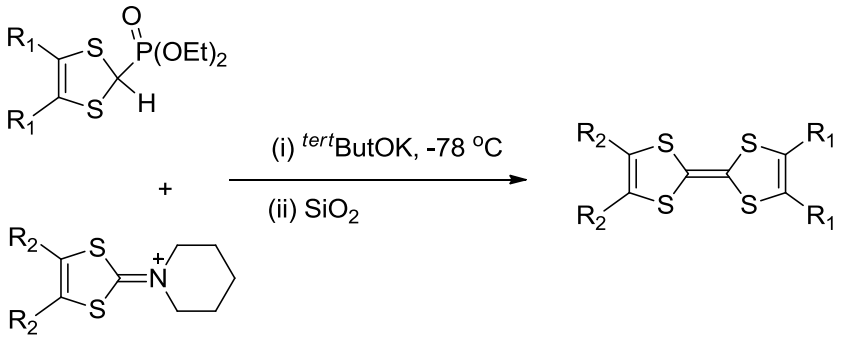

Scheme 3.3. Wittig-Horner-Emmons type condensation

In 1995, Yamada *et al.*[38] reported the synthesis of unsymmetrical TTFs *via* organometallic selective condensation (Scheme 3.4.). The reaction is based on the Lewis acid-promoted reaction of organotin compounds with esters, obtaining the best results when Me_3Al was used as a Lewis acid.

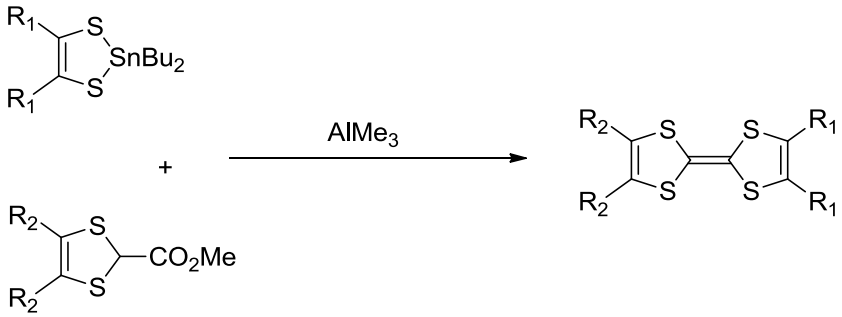

Scheme 3.4. Yamada Coupling Reaction

Another widely used method to synthesise unsymmetrical TTFs is by lithiation of the TTF core with ^{n}BuLi or LDA to form tetrathiafulvalenyllithium followed by addition of an electrophile.[39,40,41] This method allows the direct attachment of the main functional groups to the TTF core (such as aldehydes, halogens, acids, amides, ketones, esters, amines, alcohols and tin derivatives). These functional groups can consequently be derivitised, enlarging the scope of the reaction. Recently, a straightforward method to obtain aryl-substituted TTFs has been developed by palladium-catallysed direct C-H arylation.[42]

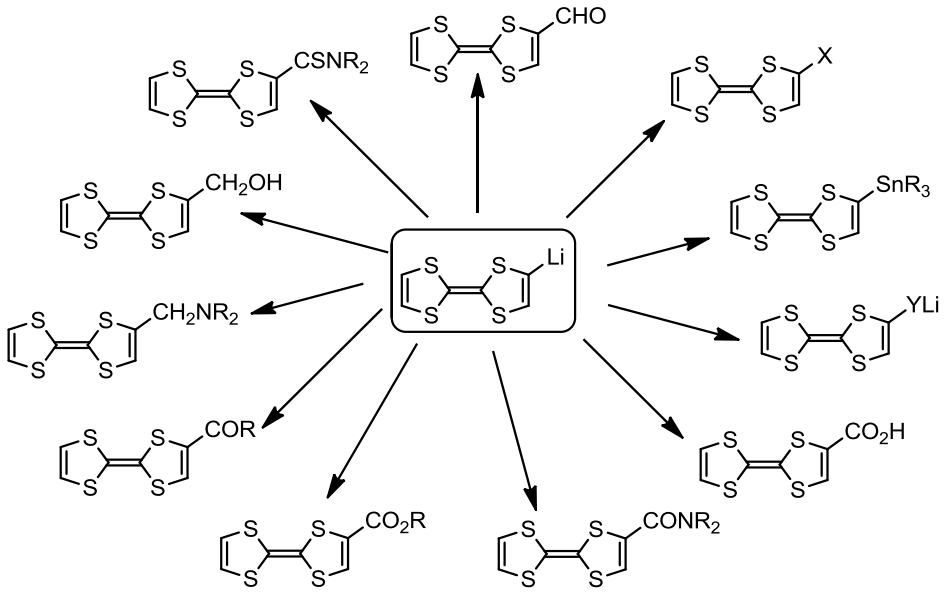

Figure 3.2. Derivatisation of tetrathiafulvaneyllithium, where X= Br, I and Y=Se, Te.

3.3.2 TTF in Polymers

Although the vast majority of the TTF derivatives have been synthesised as small molecules, there are several examples of TTF being incorporated into higher structures such as macrocycles, dendrimers, oligomers and polymers.[43,3,44,26,10] TTF units have also been incorporated into polymer backbones (see, for example **49**[45]), or even in conjugated polymers (such as **50**[46]).[47,48] Likewise, pendant TTF units have also been attached to conjugated polymers.[49,50] Interestingly, Hou *et al.* synthesised a poly(*p*-arylenenethynylene) conjugated polymer which had tethered TTF units to the main polymer chain (**51**).[49] The photovoltaic properties of this polymer were investigated in a BHJ-type-structure solar cell. In combination with PCBM (ratio polymer:PCBM 2:1), a power conversion efficiency of 0.23% was obtained.

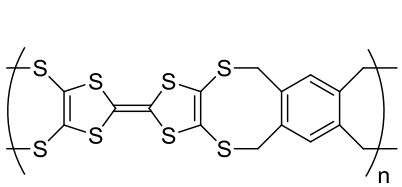

49

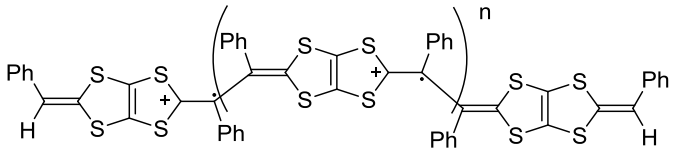

50

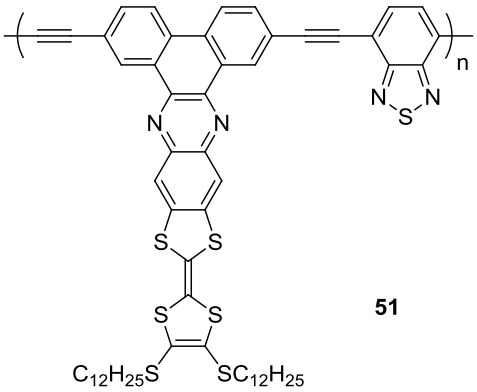

51

The incorporation of redox active species into conjugated polymers has been challenging. Electroactive units such as ferrocene, phthalocyanine and fullerenes have been attached to conjugated polymers and their properties have been widely investigated.[51,52,53,54] The study of the effects of the tethered redox species into polymers is of high importance to understand whether these units and the conjugated backbone combine their electroactivity to give hybrid properties, or that they have suppressing behaviours, or that they simply act independently.

In that sense Skabara *et al*. have focused on the direct incorporation of TTF units into polythiophene conjugated backbones. The key intermediate is the oxone derivative (**42**) of the trithiocarbonate species **40**, which enables direct combination of both electroactive families.[55] Attempts to electropolymerise **52** were unsuccessful due to the TTF unit acting as a radical scavenger, or due to the rapid reaction of the tricationic species (two reversible peaks are observed at +0.46 V and +0.83 V ascribed to the oxidation of the TTF unit to the radical cation and dication, respectively; a third irreversible peak at +2.18 V is attributed to the oxidation of the thiophene unit) with either the solvent or the anion in solution. The same group

achieved the electropolymerisation of a fused TTF-terthiophene derivative, where the TTF and the conjugated backbone were bridged by a 1,4-dithiin unit.[56]

The 2,5-dibrominated derivative of **52** was polymerised under Yamamoto conditions and the electrochemical behaviour of the resultant homopolymer (**53**) was studied in detail.[57] Spectrochemical studies (using absorption and EPR spectroscopies) showed that the incorporation of the TTF units into the conjugated backbone increases highly the degree of doping levels of polythiophene-based polymers. This fact confirmed that both electroactive species do not act independently along the material, but hybrid behaviour is obtained.

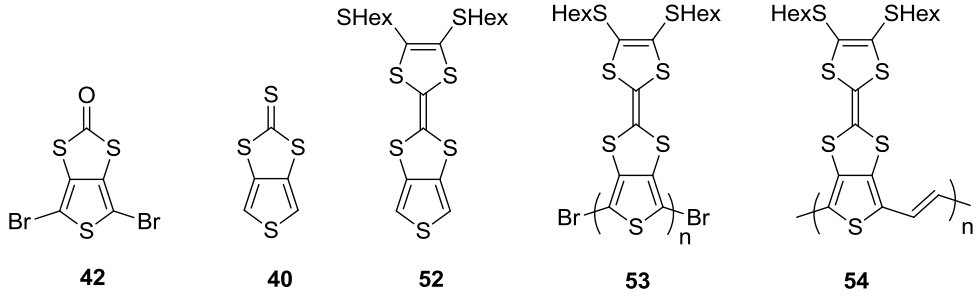

Following the interest of these TTF-thiophene hybrid materials, organic solar cells were fabricated from a polymer with vinyl groups bridging the fused TTF-thiophene units (**54**) and the photovoltaic properties were tested.[58] When the polymer was mixed in a 1:2 ratio with PCBM a power conversion efficiency of 0.13% was obtained under AM 1.5 solar simulated light. The low efficiency can be due to factors such as an inadequate match of the LUMO levels of the polymer and PCBM (see introduction)[59] and the quality of the drop-casted film.

3.4 SYNTHESIS OF MONOMERS AND p(TTF-DPP) COPOLYMER

Although single molecules of TTF derivatives have been widely used to fabricate OFETs,[11,12,13] and to a lesser extent solar cells,[19,58,49] the incorporation of TTF units

into conjugated polymers and study of their properties in organic devices remains fascinating. In that sense, following Skabara's approach to integrate the TTF core into polythiophene based-polymers, the synthesis of a copolymer based on fused thieno-TTF unit and diketopyrrolopyrrole (DPP, **55**) units was attempted.

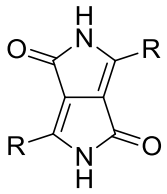

55

In the past five years the DPP unit has been extensively incorporated into the conjugated backbone of polymers as an electron-acceptor moiety.[60] The great interest of this unit relies on properties such as *(i)* large intermolecular interactions due to π-π stacking between the chains, *(ii)* formation of supramolecular order, increasing the charge carrier mobilities (electron and holes) and *(iii)* high electron and hole mobilities, which results in materials with ambipolar behaviour.[61,62,63,64,65] In order to find the best electronic properties (HOMO and LUMO levels and band gap), the DPP core has widely been derivitised with aromatic rings and copolymerised with a vast number of electron-donor moieties. These copolymers have shown good performance in devices such as OFETs and OPVs.[66,67,68,69,70,71]

Scheme 3.5. shows the synthetic route to prepare the comonomer based on a DPP core and two thiophenes attached (**35**). This route to prepare DPP units is well-known and each step was carried out following procedures found in the literature.[72] The formation of the DDP core (in this case bearing two thiophene rings) was started from 2-thiophene-carbonitrile, which was reacted with dimethyl succinate and *tert*-amyl alkoxide. After filtration and several washed with water and methanol, a highly insoluble dark-purple solid was achieved. In order to obtain a soluble processable, conjugated polymer and due to the nature of the other monomer (fused thieno-TTF, see below), long branched alkyl chains were attached to the DPP core.[73] Compound

35 was obtained by deprotonation of the lactam ring and addition of long branched bromoalkane.

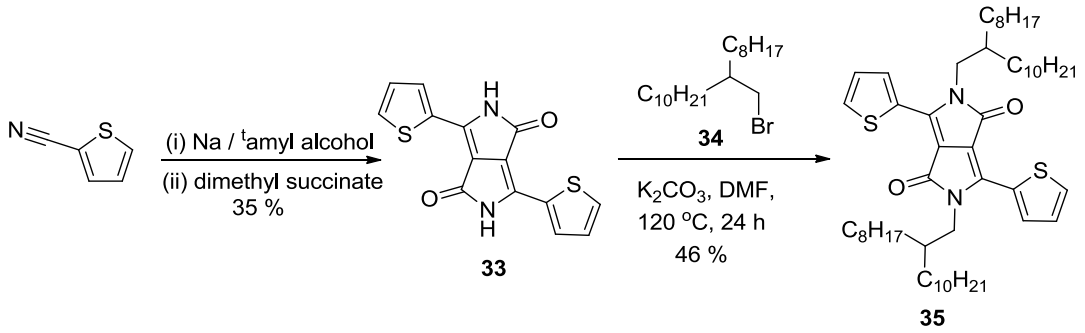

Scheme 3.5. Synthesis of compound **35**

At this stage, whereas most of the precursors of DPP-based comonomers are brominated,[61,63,64] a more suitable DPP derivative was synthesised. Following a recent procedure to prepare *in situ* a boronic ester derivative of DPP by lithium anion trapping, **35** was treated with LDA in the presence of 2-isopropoxy-4,4,5,5-tetramethyl-1,3,2-dioxoborolane to yield **36**.[74] This derivative was synthesised so that polymerisation could be carried out with the dibrominated-fused thieno-TTF derivative *via* Suzuki cross-coupling reaction.

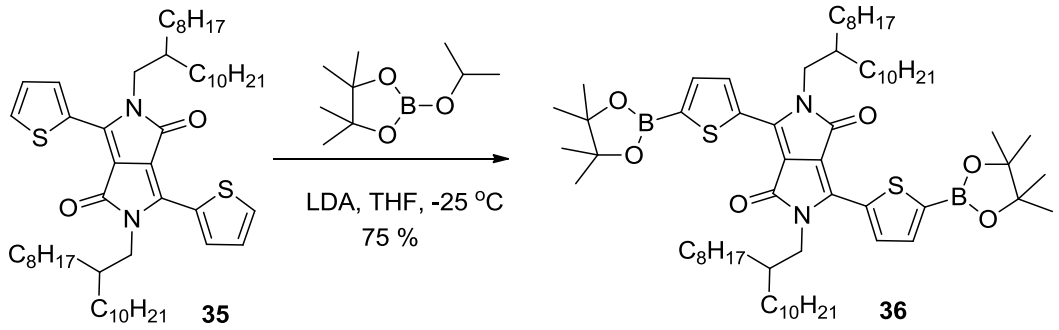

Scheme 3.6. Synthesis of compound **15**

Scheme 3.7. shows the synthetic route to prepare the comonomer based on a fused thieno-TTF derivative. The key trithiocarbonate **40**[75] was synthesised following a procedure developed by Skabara *et al.*[55] The diester **56** is reduced to the corresponding diol **37** by treatment with $NaBH_4$ and LiBr. Nucleophilic substitution

of diol with phosphorous tribromide yields the dibrominated derivative **38**. The fused thieno-TTF derivative **40** is obtained by precise cyclisation with sodium sulfide (minimising the polymer formation), followed by aromatisation with DDQ. Transchalcogenation of the thione is carried out using mercuric acetate and the subsequent one is brominated with bromine to obtain the key intermediate **42**.

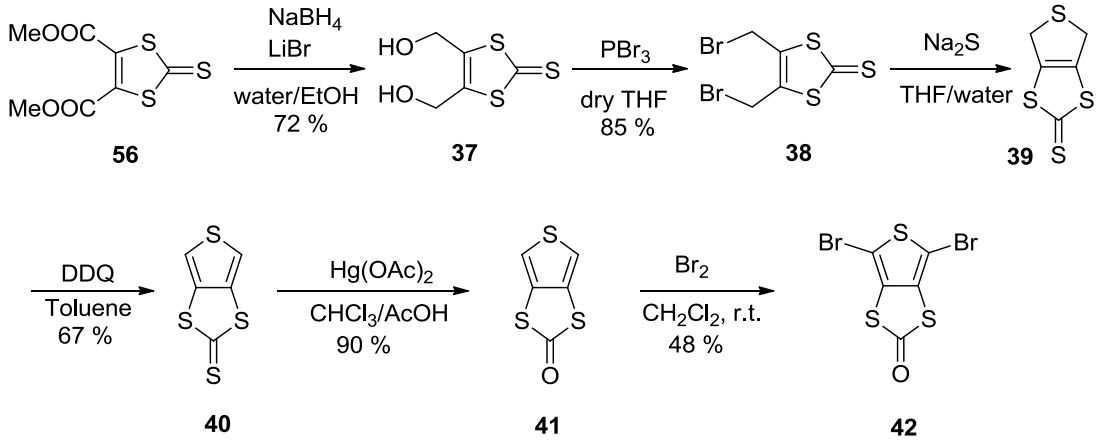

Scheme 3.7. Synthesis of compound **42**.

As reported before, X-ray crystallographic studies showed that the two hexyl chains of the monomer of homopolymer **53** are almost orthogonal to the remainder of the molecule (85.2 ^{o}C).[76] This could be detrimental towards close interchain interactions and the film-forming properties of the polymer. Therefore, the hexyl chains used in the previous compounds of the series (they were required for obtaining soluble polymers) were replaced by methyl groups **43**. Hitherto, the solubility of the polymer will be provided by the long branched alkyl chains to the DPP core. TTF-based comonomer **22** was obtained by phosphite mediated cross-coupling reaction in 63% yield.

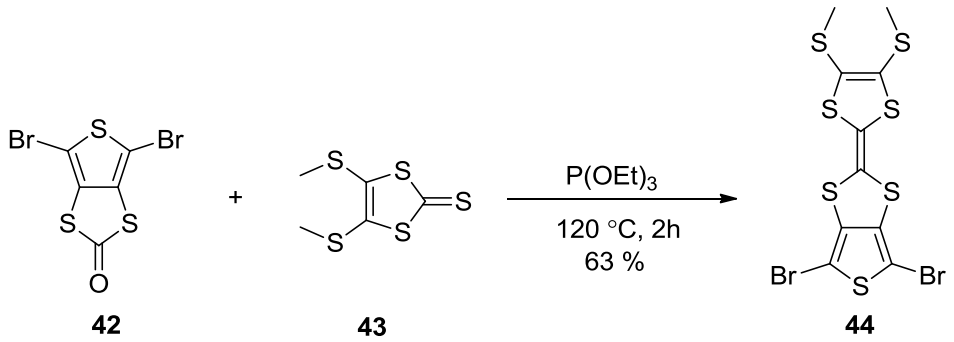

Scheme 3.8. Synthesis of compound **44**.

The polymer **p(DPP-TTF)** was synthesised by a modified Suzuki–Miyaura cross-coupling method using $Pd_2(dba)_3$ as a catalyst and potassium phosphate as a base (Scheme 3.7.). The reaction was stirred under reflux for 48 h and the polymer was end-capped with 2-bromo-thiophene and 2-thienylboronic acid. Soxhlet extractions with methanol, acetone and chloroform were carried out to give a dark-greenish polymer. The solids obtained from the chloroform fractions were used for characterisation of the polymer and for the preparation of devices (see below). The degree of polymerisation was studied by gel permeation chromatography in chlorobenzene giving a molecular weight of M_n = 9.6 kDa (P.D.I. = 3.0).

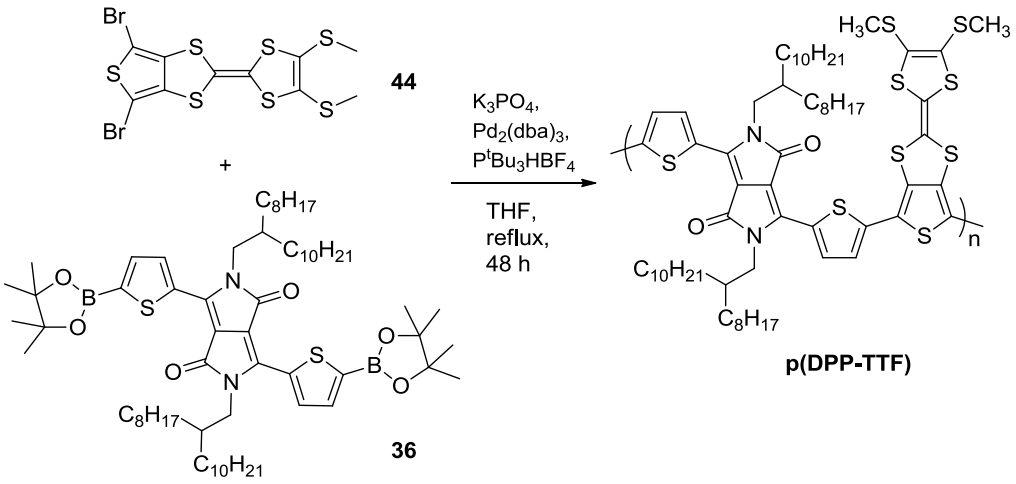

Scheme 3.9. Synthesis of compound **p(DPP-TTF)**

3.5 THERMAL PROPERTIES

Thermogravimetric analysis (TGA) was carried out in order to study the thermal stability of **p(DPP-TTF)**. The polymer showed good stability up to 300 ^{o}C. This temperature is high enough to treat the polymer thermally and obtain ordered morphologies without damaging the polymer during the preparation of devices. Differential scanning calorimetry (DSC) of p(DPP-TTF) showed evidence of a crystallisation point occurring at around 175 ^{o}C.

3.6 ELECTROCHEMICAL AND UV-VIS ABSORPTION SPECTROSCOPY OF P(DPP-TTF)

The electrochemical behaviour of **p(DPP-TTF)** was determined by cyclic voltammetry analysis, both in solution and solid-state, with *i*R compensation. The solid state studies were carried out in acetonitrile (the solvent does not dissolve the polymers) by drop-casting a solution of the polymer (in dichloromethane) onto a glassy carbon electrode, which acted as the working electrode. The experiments were carried out at a scan rate of 0.1 V/s. In both cases, a Ag wire reference electrode and a Pt counter-electrode were used. The experiments were carried out using tetrabutylammonium hexafluorophosphate (0.1 M) as the supporting electrolyte and all the values are quoted *versus* the redox potential of the ferrocene/ferrocenium couple. The oxidation and reduction graphs for each experiment were obtained independently and not as a full cycle, as the presence of irreversible peaks can give imprecise redox behaviours. Additionally, the solutions were bubbled with argon prior to each reduction process.

Figure 3.3. depicts the oxidation and reduction waves of **p(DPP-TTF)** and Table 3.1. and Table 3.2. summarise the redox behaviour. In solution, **p(DPP-TTF)** shows several oxidation processes, beginning with a well-defined wave at +0.33 V, followed by peaks at +0.56, +0.71 and +0.85 V. The first reversible oxidation peak

can be attributed to the bis(thioether)-substituted half-unit, whereas the next reversible process is ascribed to the dithiole half-unit fused to the thiophene of the polymer backbone.[58] This accounts for the classical reversible double oxidation process of the TTF unit. The assignment of the remaining peaks in the voltammogram is speculative due to the complexity of the structure, but oxidation of the terthiophene unit will certainly be taking place. The polymer shows a quasi-reversible reduction wave at -1.45 V, which is assigned to the DPP repeat unit.

The redox behaviour of **p(DPP-TTF)** in the solid state differs significantly from its behaviour in solution. Upon oxidation, the polymer shows two quasi-reversible peaks at +0.45 and +0.68 V. The first oxidation in the solid state occurs at a considerably higher potential value compared to the same process in solution. This difference in the first oxidation potential of the polymer in solution and in the solid state could be attributed to partial charge transfer between the TTF and DPP units in the solid state. Two reduction peaks are present at -1.41 and -1.76 V, respectively. The latter could well be due to the reduction of the terthiophene component of the polymer, which is less reversible than the redox wave associated with the DPP unit.

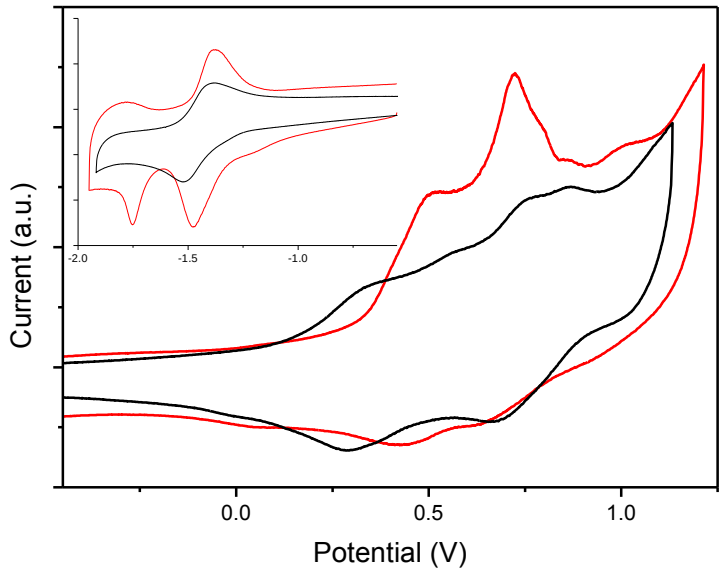

Figure 3.3. Cyclic voltammograms of **p(DPP-TTF)** in solution (black) and in solid state (red).

	Cyclic Voltammetry			
	E_{ox}/V	**E_{red}/V**	**HOMO/LUMO/ eV**	**HOMO-LUMO gap/eV**
p(DPP-TTF)	+0.37/+0.29,[r] +0.56,[i] +0.76/+0.67,[r] +0.85[i]	-1.45[qr]	-4.95/-3.55	1.40

Table 3.1. Electrochemical properties of **p(DPP-TTF)** in solution.

	Cyclic Voltammetry			
	E_{ox}/V	**E_{red}/V**	**HOMO/LUMO/eV**	**HOMO-LUMO gap/eV**
p(DPP-TTF)	+0.45,[qr] +0.68[qr]	-1.4[ir] -1.76[ir]	-5.13/-3.49	1.64

Table 3.2. Electrochemical properties of **p(DPP-TTF)** in solid state.

UV-vis spectroelectrochemical measurements were carried out on a thin film of the drop-cast polymer on an ITO slide. The film was dedoped in an acetonitrile solution in the presence of tetrabutylammonium hexafluorophosphate (0.1 M), by repetitive cycling between the first oxidation and the first reduction waves, which covers the neutral state of the polymer. The results are shown in Figure 3.4. Previous spectroelectrochemical studies of TTF derivatives show that when the first oxidation of the TTF derivative occurs, two new absorption bands are observed at 430 and 580 nm.[57,58] These bands are sometimes accompanied by an extra absorption band at around 800 nm, which is assigned to intermolecular charge transfer processes between TTF radical cations or as an additional absorption band associated with the radical cation. The second oxidation leads to the dication and the disappearance of the previous absorption bands, whilst another band at around 390 nm develops (for

the TTF dication). Using a pseudo-silver wire reference electrode, the potentials at which the peaks 390 and 600 nm appeared are around +1.0 V. These bands are assigned to the radical cations of the TTF derivatives that are produced upon oxidation. Interestingly, **p(DPP-TTF)** reveals an additional broad band that extends from around 890 nm to 1100 nm. The nature of this band is overlapped by the large absorption band of the polymer backbone, but it can be assigned to the charge transfer process that occurs from the TTF part of the polymer to the conjugated backbone when the TTF unit is oxidised.

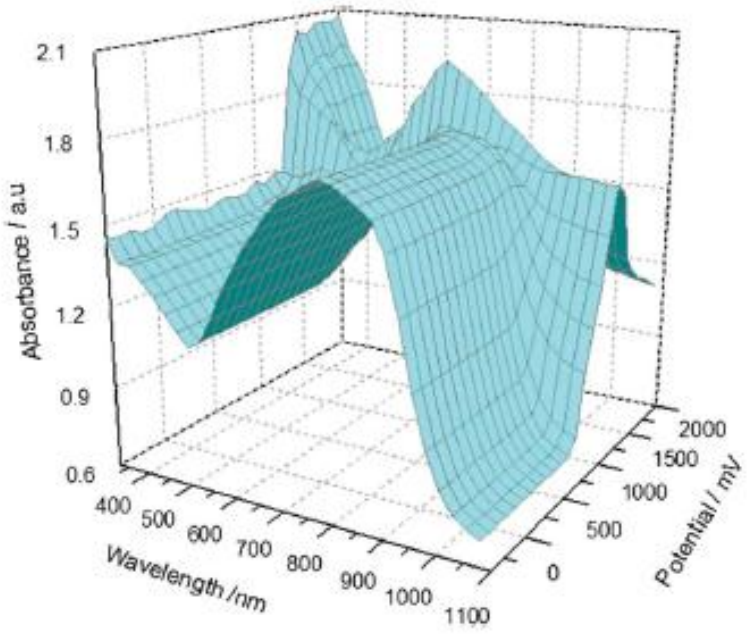

Figure 3.4. Spectroelectrochemistry of **p(DPP-TTF)**

Figure 3.5. shows the electronic absorption spectra of copolymer **p(DPP-TTF)** in solution (dichloromethane) and as a film drop-cast on indium tin oxide (ITO). All the optical data is summarised in table 3.2. In both cases the polymer has a broad absorption band from around 500 nm to 1000 nm. Due to interactions between polymer chains in the solid state, the values of the absorption maximum and the onset of the longest wavelength absorption band are bathochromically shifted compared to the solution state spectrum. In solution, the maximum absorption occurs at 769 nm, whereas in the solid state it is shifted by 17 nm.

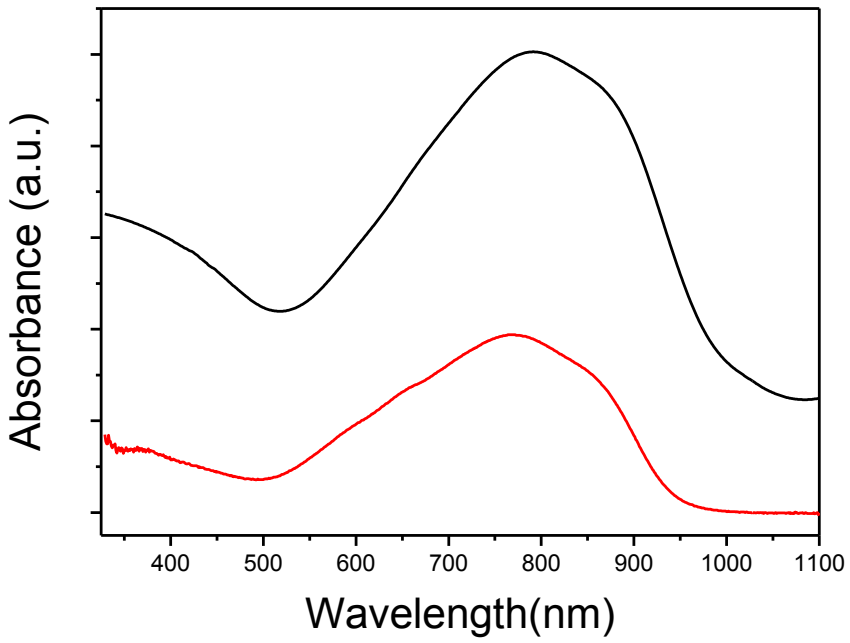

Figure 3.5. UV-vis absorption spectra of **p(DPP-TTF)** in solution (red) and in solid (black).

The onset of the optical absorption of the polymer film lies at around 1000 nm, which gives an optical band gap of 1.26 eV. In conjugated polymers, the difference between the onset of the first oxidation and the onset of the first reduction corresponds to the electrochemical band gap. As it has been stated above, the first oxidation peak of **p(DPP-TTF)** does not belong to a removal of an electron from the polymeric backbone, but from the bis(thioether)-substituted half-unit of the TTF. Therefore, the band gap we can obtain from the difference of oxidation and reduction onsets cannot be illustrative of the optical band gap of the polymer, which is inferred from the onset of the π-π* band in the absorption spectrum. The electrochemical studies carried out in solution give a HOMO–LUMO gap of 1.40 eV, whereas the gap obtained for the solid state is 1.64 eV.

On the other hand, the optical values are 1.32 eV and 1.26 eV for studies carried out in solution and in the solid state. As expected, the optical band gap in the solid state is lower than that obtained in solution due to interchain interactions. If we compare these two values with the ones obtained by electrochemistry, we see that whereas the

gap in solution is similar and within the same values, the gap in the solid state differs by more than 0.30 eV. This is not uncommon in conjugated polymers and is attributed to the structural differences in the thin film or to the exciton binding energy for conjugated polymers.[77] As stated above, stronger donor–acceptor interactions between the TTF and DPP units will arise in the solid state and this will affect the redox potentials of these two components.

	Absorption peak λ(max)/nm		**HOMO-LUMO gap / eV**	
	solution	film	solution	film
p(DPP-TTF)	769	786	1.32	1.26

Table 3.3. Optical properties and HOMO-LUMO gap of **p(DPP-TTF)**

3.7 PERFORMANCE OF p(DPP-TTF) IN OFETs AND OPVs

p(DPP-TTF) was used to fabricate OFETs and organic photovoltaics. All this work has been carried out by Mr. Sasikumar Arumugam and Dr. Anto Regis Inigo under the supervision of Professor P. J. Skabara at the University of Strathclyde. The architecture of each device is shown in the Appendix.

3.7.1. Field-effect transistor properties and surface morphology

Figure 3.6. shows the output characteristics of **p(DPP-TTF)** devices recorded at different source and drain voltages up to -80 V at intervals of 1 V, with a gate bias voltage between -10 V and -90 V at intervals of -20 V. Though these devices exhibit some hysteresis, they all have clear linear and saturation regions. Figure 3.7 shows transfer characteristics recorded at a V_{DS} of -90 V for 15 days, and for clarity, data recorded on the 1st, 8th and 15th days are shown. A saturation mobility of 4 x 10^{-2} cm^2 V^{-1} s^{-1} was calculated by fitting a straight line to V_{GS} *vs.* $(I_{DS})^{1/2}$ in the saturation

region. An on/off ratio of 1 x10^4 is also deduced from Figure 3.6. This hole mobility is similar to that of non-TTF analogues of DPP polymers already reported.[62,63,64,65]

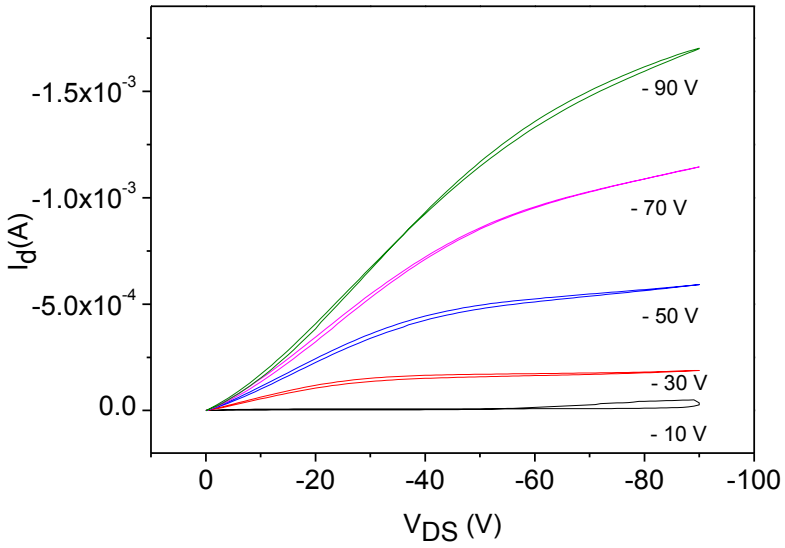

Figure 3.6. Output characteristics of **p(DPP-TTF)** measured at gate voltage intervals of 20 V.

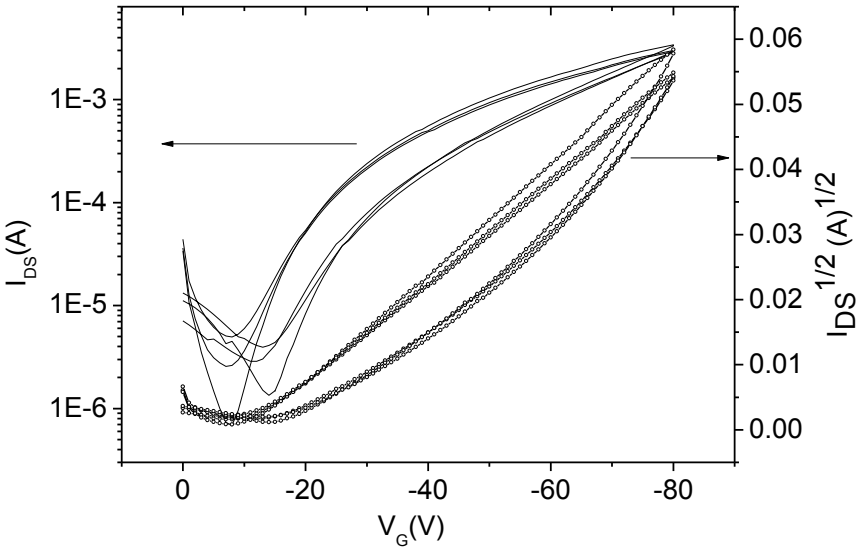

Figure 3.7. Transfer characteristics of **p(DPP-TTF)** were measured at 90 V **(**source-drain) in an ambient laboratory conditions. The data shown here were measured on the 1st, 8th and 15th days.

Figure 3.8. shows a topographic image recorded by tapping mode AFM. The representative picture was taken from the same devices used for mobility measurements. It is seen here that annealed **p(DPP-TTF)** films on octadecyltrichlorosilane (OTS) treated Si/SiO_2 substrates produce fibre-like structures upon annealing (200 ^{o}C for 20 min). Notably, DPP analogues reported to date are semi-crystalline.[62,63,64,65] Non-uniform distribution and orientation of these fibre-like structures may lead to a slightly lower mobility (of the order of ~4 x 10^{-2} cm^2 V^{-1} s^{-1}) as opposed to DPP polymer analogues that do not contain the TTF unit but have thiophene units (highest mobility of ~1 cm^2 V^{-1} s^{-1}).[62,63,64,65] Further optimisation of processing conditions for device fabrication such as the spinning process, solution concentration, and OTS treatment of SiO_2 substrates might produce higher mobilities similar to other DPP containing polymers. These device characteristics are highly reproducible under ambient laboratory conditions as shown in Figure 3.7. The stability of these devices under ambient atmospheric conditions has been attributed to the aforementioned partial charge transfer interactions between the TTF and DPP units in **p(DPP-TTF)**, which define a stable morphology and propensity of the materials to withstand the effects of an ambient environment. Moreover, the stability of the TTF unit towards oxidation is extremely well known.

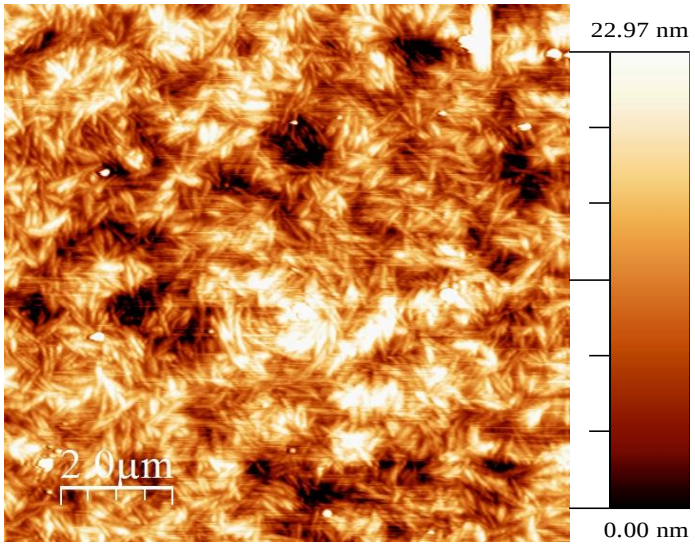

Figure 3.8. Tapping mode AFM height images of **p(DPP-TTF)** on OTS treated SiO_2 surfaces after annealing at 200 ^{o}C for 20 min.

3.8 ORGANIC PHOTOVOLTAICS

The photovoltaic properties of **p(DPP-TTF)** have been studied. In a typical bulk-heterojunction structure approach, the active layer was prepared by blending the polymer with $PC_{70}BM$. Due to the different parametres to control in order to obtain high efficiencies some early approaches have been carried out. Different **p(DPP-TTF)** concentrations of the solutions to be spin-casted have been tested, as well as the ratio polymer:$PC_{70}BM$. Although it has been shown that the addition of diiodooctane can be beneficial in order to obtain an adequate nanomorphology within the active layer, in this case no improvement was obtained. In fact the device performed worse. Figure 3.9. shows the differences of J-V characteristics for a blend of **p(DPP-TTF)**:$PC_{70}BM$ when the solution is spin-casted from dichlorobenzene and chloroform. Table 3.4 depicts the values of the short-current (I_{sc}), the open-circuit voltage (V_{oc}), fill factor (FF) and the power conversion efficiency.

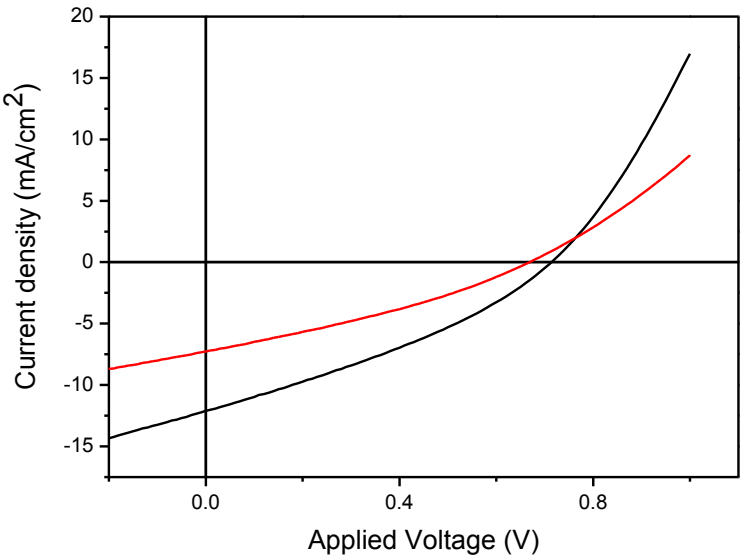

Figure 3.9. J-V characteristics for **p(DPP-TTF)**:$PC_{70}BM$ (deposited from chloroform in *red* and from dichlorobenzene in *black*) under illumination with standard AM 1.5G source.

Active layer	solvent	I_{sc} (mA/cm^2)	V_{oc} (V)	FF	PCE (%)
1:4	dichlorobenzene	12.0	0.71	0.32	2.79
1:4	chloroform	7.2	0.67	0.31	1.57

Table 3.4. Photovoltaic performance of **p(DPP-TTF)**:$PC_{70}BM$ solar cells.

The photovoltaic properties of a single component active layer have also been studied. Instead of preparing a blend of donor:acceptor as the general approach, **p(DPP-TTF)** was sandwiched between the two electrodes. Surprisingly, a remarkable power conversion efficiency of 0.46 % has been achieved so far. Figure 3.10. shows the J-V characteristics of the single component organic solar cell.

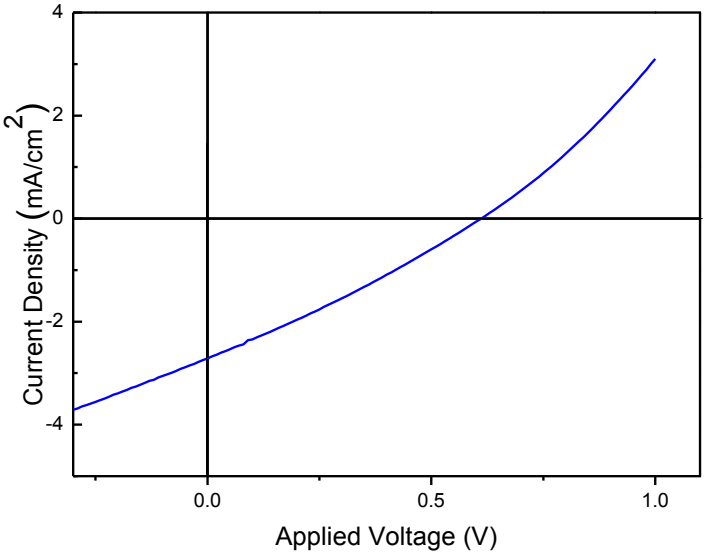

Figure 3.10. J-V characteristics for **p(DPP-TTF)** as a single component OPV.

3.9. CONCLUSIONS AND FUTURE WORK

The synthesis of a new low band polymer **p(DPP-TTF)** has been reported. The polymer is based on a fused thieno-TTF derivative which has been developed and investigated in this group. This co-monomer has been slightly changed in comparison to the other monomers of the family. In order to increase π-π stacking between the polymeric chains, the hexyl chains used in the previous examples (they lay nearly perpendicular to the thieno-TTF unit plane) were changed by methyl groups. This units was copolymerised with a bis-boronate DPP derivative *via* Suzuki cross-coupling reaction.

The polymer was fully characterised and the UV-vis absorption spectroscopy showed the high absorbance of the polymer from 500 to 1000 nm which is highly desirable for obtaining high photon harvesting properties.

p(DPP-TTF) has been studied in organic devices. The incorporation of the polymer in OFETs show a hole mobility of ~4 x 10^{-2} cm^2 V^{-1} s^{-1} with ON/OFF ratios of 10^4. It is worth noting that the hole mobility of these devices do not change remarkably during the first 15 days under ambient atmospheric conditions. This behaviour is attributed to the partial charge transfer interactions between the TTF and DPP units in **p(DPP-TTF)**.

Likewise, the photovoltaic properties of **p(DPP-TTF)** have been studied both as blend with $PC_{70}BM$ and as a single component. Early studies have shown a power conversion efficiency of 2.8 % for the BHJ-structure and 0.46 % for the single component. These values are under optimisation and higher efficiencies are expected in both devices. Additionally, in order to fully understand the reason of the remarkable efficiency of the single component as well as the high value of its V_{oc} photophysical studies are being carried at the moment.

REFERENCES

1. F. Wudl, G. M. Smith and E. J. Hufnagel, *Journal of the Chemical Society D: Chemical Communications*, 1970, 1453-1454.
2. F. Wudl, D. Wobschall and E. J. Hufnagel, *Journal of the American Chemical Society*, 1972, **94**, 670-672.
3. M. Iyoda, M. Hasegawa and Y. Miyake, *Chemical Reviews*, 2004, **104**, 5085-5114.
4. C. Rovira, *Chemical Reviews*, 2004, **104**, 5289-5318.
5. M. Bendikov, F. Wudl and D. F. Perepichka, *Chemical Reviews*, 2004, **104**, 4891-4946.
6. J.-i. Yamada, H. Akutsu, H. Nishikawa and K. Kikuchi, *Chemical Reviews*, 2004, **104**, 5057-5084.
7. D. V. Konarev, E. F. Valeev, Y. L. Slovokhotov, Y. M. Shul'ga, O. S. Roschupkina and R. N. Lyubovskaya, *Synthetic Metals*, 1997, **88**, 85-87.
8. J. Ferraris, D. O. Cowan, V. Walatka and J. H. Perlstein, *Journal of the American Chemical Society*, 1973, **95**, 948-949.
9. A. M. Kini, U. Geiser, H. H. Wang, K. D. Carlson, J. M. Williams, W. K. Kwok, K. G. Vandervoort, J. E. Thompson and D. L. Stupka, *Inorganic Chemistry*, 1990, **29**, 2555-2557.
10. *Handbook of Chalcogen Chemistry. New Perspectives in Sulfur, Selenium and Tellurium.*, Royal Society of Chemistry, Cambridge, 2007.
11. Naraso, J.-i. Nishida, D. Kumaki, S. Tokito and Y. Yamashita, *Journal of the American Chemical Society*, 2006, **128**, 9598-9599.
12. C. Moreno, R. Pfattner, M. Mas-Torrent, J. Puigdollers, S. T. Bromley, C. Rovira, J. Veciana and R. Alcubilla, *Journal of Materials Chemistry*, 2012, **22**, 345-348.
13. M. Mas-Torrent and C. Rovira, *Chemical Society Reviews*, 2008, **37**, 827-838.
14. C. W. Chu, J. Ouyang, J. H. Tseng and Y. Yang, *Advanced Materials*, 2005, **17**, 1440-1443.

15. A. Akutsu-Sato, H. Akutsu, S. S. Turner, P. Day, M. R. Probert, J. A. K. Howard, T. Akutagawa, S. Takeda, T. Nakamura and T. Mori, *Angewandte Chemie International Edition*, 2005, **44**, 292-295.
16. S. Fukuzumi, K. Ohkubo, Y. Kawashima, D. S. Kim, J. S. Park, A. Jana, V. M. Lynch, D. Kim and J. L. Sessler, *Journal of the American Chemical Society*, 2011, **133**, 15938-15941.
17. T. Avellini, H. Li, A. Coskun, G. Barin, A. Trabolsi, A. N. Basuray, S. K. Dey, A. Credi, S. Silvi, J. F. Stoddart and M. Venturi, *Angewandte Chemie International Edition*, 2012, **51**, 1611-1615.
18. C. Wang, A. S. Batsanov and M. R. Bryce, *Chemical Communications*, 2004, 578-579.
19. S. Wenger, P.-A. Bouit, Q. Chen, J. l. Teuscher, D. D. Censo, R. Humphry-Baker, J.-E. Moser, J. L. Delgado, N. Martín, S. M. Zakeeruddin and M. Grätzel, *Journal of the American Chemical Society*, 2010, **132**, 5164-5169.
20. I. Fuks-Janczarek, J. Luc, B. Sahraoui, F. Dumur, P. Hudhomme, J. Berdowski and I. V. Kityk, *The Journal of Physical Chemistry B*, 2005, **109**, 10179-10183.
21. C. Wang, Q. Chen, F. Sun, D. Zhang, G. Zhang, Y. Huang, R. Zhao and D. Zhu, *Journal of the American Chemical Society*, 2010, **132**, 3092-3096.
22. J. Bigot, B. Charleux, G. Cooke, F. o. Delattre, D. Fournier, J. l. Lyskawa, L. n. Sambe, F. o. Stoffelbach and P. Woisel, *Journal of the American Chemical Society*, 2010, **132**, 10796-10801.
23. A. J. Moore and M. R. Bryce, *Synthesis*, 1997, **1997**, 407,409.
24. A. Krief, *Tetrahedron*, 1986, **42**, 1204-1252.
25. J. M. Fabre, *Chemical Reviews*, 2004, **104**, 5133-5150.
26. J. Yamada and T. Sugimoto, *TTF Chemistry: Fundamentals and Applications of Tetrathiafulvalene*, Kodansha, 2004.
27. W. R. H. Hurtley and S. Smiles, *Journal of the Chemical Society (Resumed)*, 1926, 2263-2270.
28. G. Schukat, A. M. Richter and E. Fanghänel, *Sulfur Rep.*, 1987, **7**, 155.
29. N. Svenstrup and J. Becher, *Synthesis*, 1995, **3**, 215.

30. L. R. Melby, H. D. Hartzler and W. A. Sheppard, *The Journal of Organic Chemistry*, 1974, **39**, 2456-2458.
31. H. D. Hartzler, *Journal of the American Chemical Society*, 1970, **92**, 1412-1413.
32. R. D. McCullough, M. A. Petruska and J. A. Belot, *Tetrahedron*, 1999, **55**, 9979-9998.
33. T. Konoike, K. Namba, T. Shinada, K. Sakaguchi, G. C. Papavassiliou, K. Murata and Y. Ohfune, *Synlett*, 2001, **9**, 1476.
34. N. C. Gonnella and M. P. Cava, *The Journal of Organic Chemistry*, 1978, **43**, 369-370.
35. L. Giral, J. M. Fabre and A. Gouasmia, *Tetrahedron Letters*, 1986, **27**, 4315-4318.
36. J. M. Fabre, S. Chakroune, A. Javidan, L. Zanik, L. Ouahab, S. Golhen and P. Delhaes, *Synthetic Metals*, 1995, **70**, 1127-1129.
37. K. Lerstrup, I. Johannsen and M. Jørgensen, *Synthetic Metals*, 1988, **27**, 9-13.
38. J.-i. Yamada, Y. Amano, S. Takasaki, R. Nakanishi, K. Matsumoto, S. Satoki and H. Anzai, *Journal of the American Chemical Society*, 1995, **117**, 1149-1150.
39. D. C. Green, *Journal of the Chemical Society, Chemical Communications*, 1977, 161-162.
40. D. C. Green, *The Journal of Organic Chemistry*, 1979, **44**, 1476-1479.
41. J. Garin, *Adv. Heterocycl. Chem*, 1995, **62**, 249.
42. Y. Mitamura, H. Yorimitsu, K. Oshima and A. Osuka, *Chemical Science*, 2011, **2**, 2017-2021.
43. G. Fernández, E. M. Pérez, L. Sánchez and N. Martín, *Angewandte Chemie International Edition*, 2008, **47**, 1094-1097.
44. M. Hardouin-Lerouge, P. Hudhomme and M. Salle, *Chemical Society Reviews*, 2011, **40**, 30-43.
45. R. L. Meline, I. T. Kim, J. Chen, S. Basak and R. L. Elsenbaumer, 1998, **215**, U374.

46. H. Muller, F. Salhi, T. Narayanan, M. Lorenzen and C. Ferrero, *Chemical Communications*, 1999, 1407-1408.
47. S. Frenzel, S. Arndt, R. M. Gregorious and K. Mullen, *Journal of Materials Chemistry*, 1995, **5**, 1529-1537.
48. T. Yamamoto and T. Shimizu, *Journal of Materials Chemistry*, 1997, **7**, 1967-1968.
49. Y. Hou, Y. Chen, Q. Liu, M. Yang, X. Wan, S. Yin and A. Yu, *Macromolecules*, 2008, **41**, 3114-3119.
50. Y. Liu, C. Wang, M. Li, G. Lai and Y. Shen, *Macromolecules*, 2008, **41**, 2045-2048.
51. I. Manners, *Synthetic Metal-Containing Polymers*, Wiley-VCH, Weinheim (Germany), 2004.
52. G. Sonmez, C. K. F. Shen, Y. Rubin and F. Wudl, *Advanced Materials*, 2005, **17**, 897-900.
53. T. Hasobe, P. V. Kamat, M. A. Absalom, Y. Kashiwagi, J. Sly, M. J. Crossley, K. Hosomizu, H. Imahori and S. Fukuzumi, *The Journal of Physical Chemistry B*, 2004, **108**, 12865-12872.
54. T. Benincori, E. Brenna, F. Sannicolò, L. Trimarco, P. Sozzani and G. Zotti, *Angewandte Chemie International Edition in English*, 1996, **35**, 648-651.
55. P. J. Skabara and K. Müllen, *Synthetic Metals*, 1997, **84**, 345-346.
56. P. J. Skabara, D. M. Roberts, I. M. Serebryakov and C. Pozo-Gonzalo, *Chemical Communications*, 2000, 1005-1006.
57. P. J. Skabara, R. Berridge, E. J. L. McInnes, D. P. West, S. J. Coles, M. B. Hursthouse and K. Mullen, *Journal of Materials Chemistry*, 2004, **14**, 1964-1969.
58. R. Berridge, P. J. Skabara, C. Pozo-Gonzalo, A. Kanibolotsky, J. Lohr, J. J. W. McDouall, E. J. L. McInnes, J. Wolowska, C. Winder, N. S. Sariciftci, R. W. Harrington and W. Clegg, *The Journal of Physical Chemistry B*, 2006, **110**, 3140-3152.
59. M. C. Scharber, D. Mühlbacher, M. Koppe, P. Denk, C. Waldauf, A. J. Heeger and C. J. Brabec, *Advanced Materials*, 2006, **18**, 789-794.

60. W. K. Chan, Y. Chen, Z. Peng and L. Yu, *Journal of the American Chemical Society*, 1993, **115**, 11735-11743.
61. L. Bürgi, M. Turbiez, R. Pfeiffer, F. Bienewald, H.-J. Kirner and C. Winnewisser, *Advanced Materials*, 2008, **20**, 2217-2224.
62. J. C. Bijleveld, A. P. Zoombelt, S. G. J. Mathijssen, M. M. Wienk, M. Turbiez, D. M. de Leeuw and R. A. J. Janssen, *Journal of the American Chemical Society*, 2009, **131**, 16616-16617.
63. S. Cho, J. Lee, M. Tong, J. H. Seo and C. Yang, *Advanced Functional Materials*, 2011, **21**, 1910-1916.
64. Y. Li, S. P. Singh and P. Sonar, *Advanced Materials*, 2010, **22**, 4862-4866.
65. P. Sonar, S. P. Singh, Y. Li, M. S. Soh and A. Dodabalapur, *Advanced Materials*, 2010, **22**, 5409-5413.
66. L. Biniek, B. C. Schroeder, C. B. Nielsen and I. McCulloch, *Journal of Materials Chemistry*, 2012.
67. T. L. Nelson, T. M. Young, J. Liu, S. P. Mishra, J. A. Belot, C. L. Balliet, A. E. Javier, T. Kowalewski and R. D. McCullough, *Advanced Materials*, 2010, **22**, 4617-4621.
68. Z. Chen, M. J. Lee, R. Shahid Ashraf, Y. Gu, S. Albert-Seifried, M. Meedom Nielsen, B. Schroeder, T. D. Anthopoulos, M. Heeney, I. McCulloch and H. Sirringhaus, *Advanced Materials*, 2012, **24**, 647-652.
69. M. Shahid, T. McCarthy-Ward, J. Labram, S. Rossbauer, E. B. Domingo, S. E. Watkins, N. Stingelin, T. D. Anthopoulos and M. Heeney, *Chemical Science*, 2012, **3**, 181-185.
70. S. Qu and H. Tian, *Chemical Communications*, 2012, **48**, 3039-3051.
71. H. Bronstein, Z. Chen, R. S. Ashraf, W. Zhang, J. Du, J. R. Durrant, P. Shakya Tuladhar, K. Song, S. E. Watkins, Y. Geerts, M. M. Wienk, R. A. J. Janssen, T. Anthopoulos, H. Sirringhaus, M. Heeney and I. McCulloch, *Journal of the American Chemical Society*, 2011, **133**, 3272-3275.
72. B. Tieke, A. R. Rabindranath, K. Zhang and Y. Zhu, *Beilstein Journal of Organic Chemistry*, 2010, **6**, 830-845.

73. X. Zhang, L. J. Richter, D. M. DeLongchamp, R. J. Kline, M. R. Hammond, I. McCulloch, M. Heeney, R. S. Ashraf, J. N. Smith, T. D. Anthopoulos, B. Schroeder, Y. H. Geerts, D. A. Fischer and M. F. Toney, *Journal of the American Chemical Society*, 2011, **133**, 15073-15084.

74. H. Bürckstümmer, A. Weissenstein, D. Bialas and F. Würthner, *The Journal of Organic Chemistry*, 2011, **76**, 2426-2432.

75. P. Shu, L. Chiang, T. Emge, D. Holt, T. Kistenmacher, M. Lee, J. Stokes, T. Poehler, A. Bloch and D. Cowan, *Journal of the Chemical Society, Chemical Communications*, 1981, 920-921.

76. P. J. Skabara, K. Mullen, M. R. Bryce, J. A. K. Howard and A. S. Batsanov, *Journal of Materials Chemistry*, 1998, **8**, 1719-1724.

77. I. H. Campbell, T. W. Hagler, D. L. Smith and J. P. Ferraris, *Physical Review Letters*, 1996, **76**, 1900-1903.